Turk J Pharm Sci
DOI: 10.4274/tjps.galenos.2026.80025

ORIGINAL ARTICLE

Tannic Acid and Copper-Modified ZIF-8 Metal Organic Framework as a Cefotaxime Delivery System for Antimicrobial Activity

Yağmur PİRİNÇÇİ TOK[1]*, Münteha ÖZSOY[2], Damla DAMAR ÇELİK[3]

[1]İstanbul Health and Technology University Faculty of Pharmacy, Department of Pharmaceutical Technology, İstanbul, Türkiye
[2]Kocaeli Health and Technology University Faculty of Pharmacy, Department of Pharmaceutical Toxicology, Kocaeli, Türkiye
[3]Marmara University Faculty of Pharmacy, Department of Pharmaceutical Microbiology, İstanbul, Türkiye

ABSTRACT

Objectives: Antibiotic resistance has become a global public health threat. Cefotaxime (CTX), a third-generation cephalosporin, is approved for use in infants, children, and adults with various microbial infections, particularly those affecting the central nervous system. This study aimed to synthesize and characterize zeolitic imidazolate framework (ZIF)-8-based drug delivery systems (DDSs) to enhance antimicrobial activity and control CTX release.

Materials and Methods: ZIF-8 was synthesized via the coordination network of Zn ions and 2-methylimidazole and subsequently modified with tannic acid (TA) and copper ions (Cu^{2+}). ZIF-8 MOF and its derivatives were characterized by Fourier Transform Infrared, zeta potential, *in vitro* dissolution rate, and *in vitro* antimicrobial activity.

Results: The drug loading capacity and encapsulation efficiency were found to be 39.50 ± 1.19% and 98.75 ± 2.96%, respectively, for ZIF-8@TA@CTX, and 40.75 ± 1.22% and 97.75 ± 2.93%, respectively, for ZIF-8@TA@Cu@CTX. Following 48 hours, the drug released from ZIF-8@TA@Cu@CTX was detected at 62.83 ± 1.89% at pH 5.0 and 83.19 ± 2.50% at pH 7.4 after 48 h, with dissolution profiles best fitting the Korsmeyer–Peppas model. The synthesized DDSs demonstrated a higher antibacterial activity against gram-positive bacteria than against gram-negative bacteria.

Conclusion: ZIF-8 MOF DDs may serve as an alternative for delivering drugs to infected areas due to their controlled release under low pH conditions.

Keywords: Antibiotic resistance, metal organic framework, zeolitic imidazolate frameworks, cefotaxime

INTRODUCTION

Antibiotic resistance has become a global public health burden.[1] Each year, 700.000 people worldwide lose their lives due to antibiotic resistance, and this critical issue is predicted to cause more than 10 million annual deaths by 2050.[2] In addition to the misuse and overuse of antibiotics in humans, antibiotic resistance can occur naturally, through hereditary changes in bacterial strains, or via the transfer of resistant genes between bacteria.[3,4]

Cefotaxime (CTX) is a member of the third-generation cephalosporin group of antibiotics with greater activity against both gram-negative and gram-positive bacteria than the first and second generations.[5] It exhibits activity by preventing the biosynthesis of peptidoglycan, which is involved in the formation of the bacterial cell wall.[6] The Food and Drug Administration has approved its use for infants, children, and adults with various microbial infections, including those affecting the central nervous system, lower respiratory tract, bone and joint, genitourinary, and skin systems.[7,8] Specifically, the World Health Organization has offered it as an essential medicine for treating life-threatening meningitis.[9] However, extended-spectrum β-lactamase has been reported as a

***Correspondence:** yagmur.tok@istun.edu.tr, **ORCID-ID:** orcid.org/0000-0001-6915-0283
Received: 13.09.2025 , **Accepted:** 05.03.2026 **Epub:** 10.04.2026

Cite this article as: Pirinççi Tok Y, Özsoy M, Damar Çelik D. Tannic acid and copper-modified ZIF-8 metal organic framework as a cefotaxime delivery system for antimicrobial activity. Turk J Pharm Sci. [Epub Ahead of Print]

resistance mechanism of bacteria against third-generation cephalosporins (e.g., cefotaxime).[10]

Using nanomaterials as drug delivery systems (DDSs) to combat antibacterial resistance has been of growing interest.[11] A number of strategies based on nanomaterials, including nanoparticles and nanosystems based on metals and carbon, have been preferred to overcome the challenges of current antibiotic therapies[12] due to their large surface area, enhanced intracellular penetration, and multidrug combination.[13] Furthermore, surface modification of nanosystems enables them to target the infected site, thereby enhancing cell internalization and minimizing systemic exposure.[14]

Metal-organic frameworks (MOFs) are highly porous coordination systems comprising metal-ion nodes and organic ligands.[15] Their high surface-to-volume ratio, greater drug loading (DL) capacity, tunable surfaces, and biocompatible properties make them attractive DDSs.[16] Recently, MOFs have been applied in the literature for advanced antibacterial therapy, and this success can be attributed to different strategies. The MOF structure can consist of different metal ions, such as zinc, silver, iron, and copper. Therefore, bacterial growth can be prevented due to the antibacterial properties of these ions.[17] Furthermore, organic ligands, such as porphyrins, show photocatalytic activity with the help of light, thus facilitating the death of bacteria by forming reactive oxygen species. Lastly, MOFs can load cargo with many antibacterial activities, including drugs and antimicrobial peptides, which are triggers to kill bacteria.[18]

Zeolitic imidazolate frameworks (ZIFs) are a subclass of MOFs composed of tetrahedrally coordinated metal ions linked by imidazolate ligands. This results in the formation of zeolite-like structures. ZIF-8, constructed from zinc ions (Zn^{2+}) and 2-methylimidazolate linkers, is one of the most widely investigated ZIF materials due to its high porosity, structural stability, and pH-responsive degradation behavior, which render it attractive for drug delivery applications.[19] For instance, Costa et al.[2] combined ZIFs and zinc oxide (ZnO) nanoparticles to increase ciprofloxacin activity and provide its controlled release. The DL process was conducted following the incorporation of ZnO with ZIF-8. The resultant complex (CIP-ZnO@ZIF-8) demonstrated significantly elevated activity, exhibiting 10- and 200-fold higher activity against the *Staphylococcus aureus* strain and *Pseudomonas aeruginosa*, respectively.

Tannic acid (TA) is a natural secondary compound found in numerous plants and has various pharmacological activities, including anti-tumor, anti-diabetes, anti-obesity, and anti-myocardial ischemia.[20] Recently, TA has been encapsulated in different nanoscale DDSs to increase its antimicrobial (e.g., antiviral, antibacterial, and antifungal) and anti-inflammatory activities.[21]

In 2008, the Environmental Protection Agency approved copper (Cu^{2+} ions) as the pioneer metallic antimicrobial agent, which can kill bacteria at a rate of 99.9%.[22] Cu ions penetrate the bacterial cell membrane, enter the cell via transport proteins following membrane rupture, and bind to essential components such as DNA and proteins. This results in cell death and antibacterial activity.[23]

The current study aimed to investigate the efficacy of ZIF-8 (ZIF-8@TA@Cu@CTX), a TA- and Cu-functionalized material, in enhancing the antibacterial activity and controlling the release of CTX. For this purpose, ZIF-8 was synthesized by a one-pot method and functionalized with TA and Cu, which may contribute to a reduction in the dose of CTX due to their inherent antibacterial properties. The synthesis of ZIF-8 was confirmed by X-ray diffraction, thermogravimetric analysis, and scanning electron microscopy, and the structure of its derivatives was verified by Fourier Transform Infrared (FT-IR) analysis. ZIF-8, ZIF-8@TA, ZIF-8@TA@Cu, ZIF-8@TA@CTX, and ZIF-8@TA@Cu@CTX were subjected to *in vitro* antibacterial tests to investigate and compare their antibacterial activity. Finally, the *in vitro* drug release behavior in the dissolution media, namely acetate buffer (pH 5.0) and phosphate buffer (pH 7.4), was evaluated.

MATERIALS AND METHODS

Materials

Zinc nitrate hexahydrate [$Zn(NO_3)_2.6H_2O$], 2-methylimidazole (2-MeIm), TA, and copper (II) sulfate pentahydrate ($CuSO_45H_2O$) were obtained from Sigma-Aldrich. Methanol (MeOH) and dimethyl sulfoxide (DMSO) were obtained from MERCK Millipore, Germany. A Sartorius Arium Pro purification system was used to supply ultrapure water.

Synthesis of the ZIF-8

ZIF-8 was produced according to the ratio reported by Özsoy et al.[24] 1.35 g of $Zn(NO_3)_2{\cdot}6H_2O$ and 0.75 g of 2-MeIm were dissolved in 30 mL of MeOH separately. The latter solution was added dropwise to the zinc nitrate solution, and the mixture was stirred for 1 h. Finally, ZIF-8 complexes were obtained by washing with MeOH after for centrifugation at 4000 rpm for 15 minutes, and this procedure was performed three times.

Modification of ZIF-8 using TA and Cu

TA and copper sulfate solutions were prepared separately to modify the ZIF-8 surface; 0.5 g of TA was dissolved in deionized distilled water (DDW), and 0.2 g of ZIF-8 was dispersed in MeOH. TA solution was added dropwise to the ZIF-8 dispersion to form ZIF-8@TA, and stirring was continued for 2 h. The mixture was centrifuged at 4000 rpm for 15 min and washed with MeOH to obtain the final product (ZIF-8@TA). This process was repeated three times. ZIF-8@TA was dispersed in MeOH, and copper sulfate solution (0.2 g in DDW) was added dropwise to synthesize ZIF-8@TA@Cu. The same centrifugation and washing procedures described above were applied.

Synthesis of ZIF-8@TA@CTX and ZIF-8@TA@Cu@CTX

The drug-to-delivery system ratio was adjusted to 1:2.5.[24] The CTX solution in DMSO was added dropwise to the ZIF-8@TA and ZIF-8@TA@Cu dispersions separately for each dispersion. The necessary steps to obtain the final products were performed following a 1-day stirring period at room temperature, as mentioned above.

DLC and EC of ZIF-8@TA@Cu@CTX

The amount of CTX loaded into the designed DDSs was determined using the standard curve at 260 nm ultraviolet–visible (UV–Vis) spectroscopy.[8] Equations (1) and (2) were used to calculate the CTX loading capacity (%) and EE (%).[25]

$$\text{DL capacity (\%)} = \frac{\text{Amount of drug in carrier (mg)}}{\text{Amount of carrier (mg)}} \times 100 \quad (1)$$

$$\text{Encapsulation efficiency (\%)} = \frac{\text{Amount of drug in carrier (mg)}}{\text{Amount of drug added initially}} \times 100 \quad (2)$$

In vitro dissolution rate studies from designed DDS

To evaluate the drug release behavior of the designed ZIF-8@TA@Cu@CTX, *in vitro* dissolution rate studies were conducted in two distinct media (acetate, pH 5.0, and phosphate buffer, pH 7.4). ZIF-8@TA@Cu@CTX was selected as a representative formulation for dissolution kinetics studies because the incorporation of Cu^{2+} was anticipated a priori to have the greatest impact on both the coordination environment and release behavior. A specific quantity of sample used in drug release studies was dispersed individually in 10 mL of pH 5.0 and pH 7.4 buffers via sonication and subsequently sealed within dialysis bags. These bags were then immersed individually in 50 mL of the corresponding pH buffer and agitated at 37 °C using a magnetic stirrer set to 200 rpm for a duration of 48 hours. At periodic intervals, 1 mL of the sample was taken for analysis and replaced with a fresh buffer solution to ensure the maintenance of sink conditions. The drug amounts in the samples collected from the release medium were determined using UV-Vis at 260 nm wavelength. Following the determination of the drug's release at the point of interest, numerous mathematical models, such as zero-order, first-order, Higuchi, and Korsmeyer–Peppas have been used to evaluate the release profiles. The equations for each model are given below. The parameter k represents each model's rate constant, n indicates the release exponent, and Q represents the amount of drug dissolved at time t.[26]

$$\begin{aligned} Q_t &= k_0 \cdot t \\ Q_t &= Q_0 \cdot (1 - e^{-k_1 \cdot t}) \\ Q_t &= k_H \cdot \sqrt{t} \\ Q_t &= k \cdot t^n \end{aligned} \quad (3)$$

Characterization studies

To identify the functional groups and determine the structural characterization of the ZIF-8, ZIF-8@TA, ZIF-8@TA@Cu, ZIF-8@TA@CTX, and ZIF-8@TA@Cu@CTX samples, FT-IR analysis was conducted on a Perkin Elmer instrument in the range of 4000–400 cm^{-1}. Characteristic peaks were evaluated from the obtained spectra, and the chemical structure was confirmed.

The zeta potential, particle size, and polydispersity index (PDI) of rehydrated samples were measured using a Zetasizer Nano ZS (Malvern Instruments, Malvern, UK). Zeta potential measurements were performed after rehydration in buffer solutions at a defined concentration, whereas particle size measurements were conducted following rehydration in deionized water.[27]

Minimum inhibitory concentration (MIC) and minimum bactericidal concentration (MBC)

This assay involves determining the antimicrobial susceptibility spectrum of compounds according to the resistance of gram-positive and gram-negative bacteria using the Clinical and Laboratory Standards Institute (CLSI) broth microdilution method. The MIC is the lowest concentration of molecules that completely inhibits visible growth. The antimicrobial properties of the solvents were assessed to serve as a control, and the results of the tests were evaluated in accordance with established protocols.[28] Bacterial inocula were prepared from overnight cultures to achieve concentrations of 1 x 10^8 colony forming units (CFU)/mL. Mueller–Hinton broth (Oxoid) was used to determine the MIC, while tryptic soy agar (TSA, Difco Laboratories) was used to evaluate the MBC value.

The MBC refers to the lowest concentration of antimicrobial agents required to attain a 99.9% reduction in the initial inoculum, as quantified by CFU counts. 10 µL samples were extracted from each well of the microplate and transferred to TSA-containing Petri dishes. After a 24-h incubation period at 37 °C, the colonies were inspected to ascertain the presence of MBC.[29] The positive control wells contained bacteria without any drugs, and the negative control wells contained only the media and were used to confirm the sterility of the medium. The tests were performed using standard antibacterial agents, such as meropenem and ciprofloxacin, as controls.[28]

Statistical analysis

The data obtained from *the in vitro* dissolution studies were statistically analyzed through non-linear regression using the GraphPad Prism 9.0 statistical program. The microbiological results were interpreted in accordance with the sensitivity limits established by recognized authorities, such as the CLSI or the European Committee on Antimicrobial Susceptibility Testing. Because MIC is not a continuous variable, statistical analysis is not required for MIC testing. All characterization tests except for FT-IR analysis were performed in triplicate (n = 3). Standard deviations presented where applicable. In the antimicrobial tests, standard deviations were not reported when identical concentration values were obtained across replicates. This information has been clarified in the revised manuscript.

RESULTS

ZIF-8 was synthesized via coordination polymerization and modified with TA and Cu, respectively. After these modifications, CTX was separately loaded on ZIF-8@TA and ZIF-8@TA@Cu to evaluate their antimicrobial activity as DDSs, as shown in Figure 1.

In the ZIF-8 spectrum (Figure 2), the first stretching peak at 3200 cm^{-1} was due to the N-H bond, and the other small peaks at 3100 and 2800 cm^{-1} could be attributed to the imidazole ring and methyl group, respectively.[30] The peaks at 1450 and 1560 cm^{-1} were determined to be due to the C=N stretching modes from 2-Melm, whereas the peak at 1380 cm^{-1} was attributed to the entire ring stretching. The stretching peak that appeared

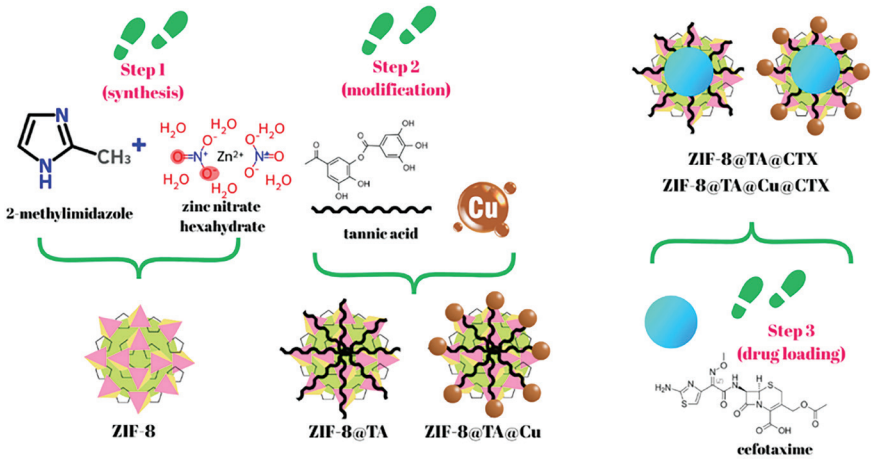

Figure 1. Synthesis of ZIF-8@TA, ZIF-8@TA@Cu, ZIF-8@TA@CTX, and ZIF-8@TA@Cu@CTX.
CTX, cefotaxime; TA, tannic acid; ZIF, zeolitic imidazolate framework.

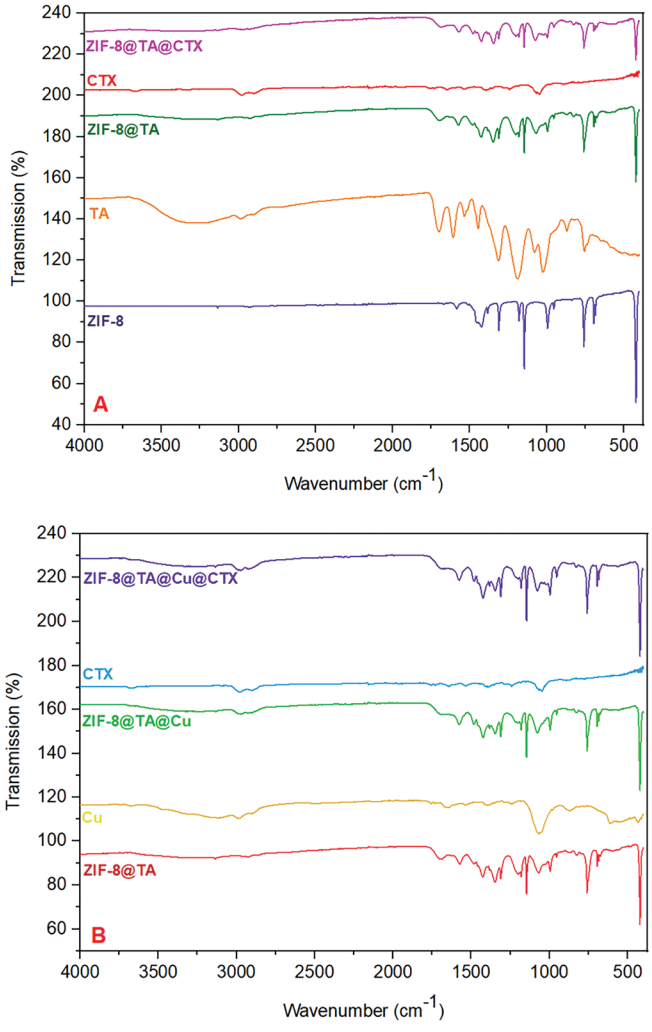

Figure 2. FT-IR spectra of the synthesized DDSs A (ZIF-8@TA@CTX synthesis steps) and B (ZIF-8@TA@Cu@CTX synthesis steps).
CTX, cefotaxime; DDSs, drug delivery systems; FT-IR, Fourier Transform Infrared; TA, tannic acid; ZIF, zeolitic imidazolate framework.

at 1000 cm^{-1} was due to C-N bond of imidazole, and the peaks ranging from 1100 to 900 cm^{-1} could be related to the in-plane bending of the ring. The peak observed at 420 cm^{-1} confirmed the formation of the ZIF-8 structure due to the Zn-N bond formed as a result of the reaction between 2-MeIm and Zn atoms.[24] In the TA spectrum, a broad band ranging from 3500–3200 cm^{-1} was attributed to the stretching vibration of O-H groups, while the peaks at 2900–2800 cm^{-1} were associated with C-H stretching vibrations of CH_2 and CH_3, respectively. The stretching vibrations of C=O from the carbonyl group located at 1700 cm^{-1}, which confirms aromatic ester moieties.[31] The ZIF-8@TA spectrum show broad O–H (≈3300 cm^{-1}) and C–O (≈1210/1040 cm^{-1}) bands characteristic of TA. The C=O band of TA was weaker and shifted ~20 cm^{-1} downwards relative to TA, and a shift of around 4 cm^{-1} was observed in the Zn–N band. These findings indicate that the phenolic groups were bound via Zn^{+2} surface coordination/H-bonding. The appearance of β-lactam C=O (~1700 cm^{-1}), amide I (~1600 cm^{-1}) and amide II (~1560 cm^{-1}) bands specific to CTX in the spectrum of ZIF-8@TA@CTX, the displacement of C–O bands of TA (≈1210/1040 cm^{-1}) and the preservation of ZIF-8 backbone bands (and ~420 cm^{-1}) indicate that CTX was successfully immobilized on ZIF-8@TA. The spectrum of ZIF-8@TA@Cu showed a decrease in the width of the TA O–H band and a downward shift of the C–O bands (≈1210/1040 cm^{-1}) by ≈12 cm^{-1}, as well as the appearance of a new, weak Cu–O band around 615 cm^{-1} and the preservation of the ZIF-8 skeleton bands (e.g. ≈420 cm^{-1}), indicate that Cu^{2+} is coordinatively bound to the surface via TA. Similar to ZIF-8@TA@CTX, characteristic peaks belonging to CTX were also observed in the ZIF-8@TA@Cu@CTX spectrum.

The surface charges of ZIF-8 and its derivatives were examined by zeta potential measurement, as shown in Figure 3. ZIF-8 exhibited a negative surface charge in acetate buffer (pH 5.0) and phosphate buffer (pH 7.4), in line with the literature.[32] The analysis of particle size and PDI performed on rehydrated formulations revealed hydrodynamic diameters in the micron range (2380 ± 209 nm and PDI: 0.24 ± 0.04 for ZIF-8@TA@

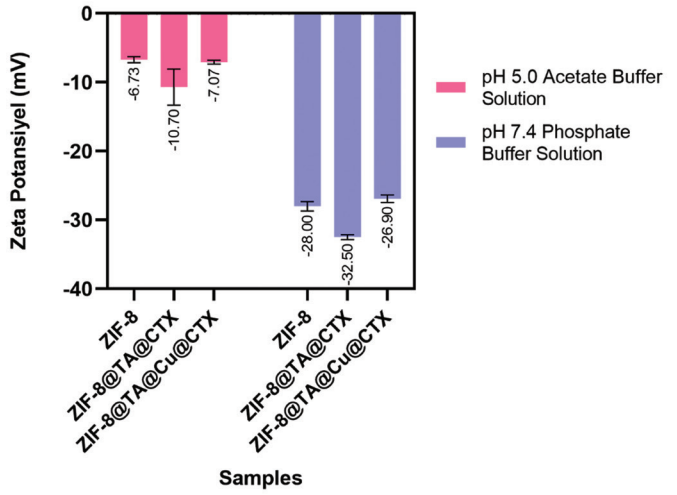

Figure 3. Zeta potential of ZIF-8 MOF and its derivatives in aqueous buffer solutions.

CTX, cefotaxime; MOF, metal-organic frameworks; TA, tannic acid; ZIF, zeolitic imidazolate framework.

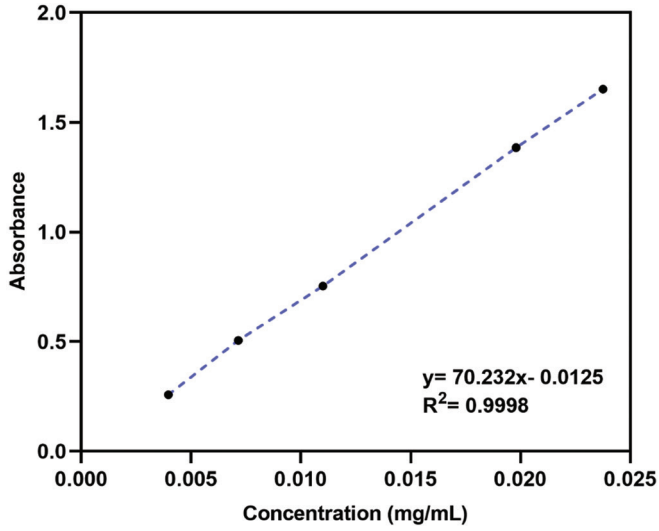

Figure 4. Standard curve of CTX for EE and DL evaluation.

CTX, cefotaxime; DL, drug loading; EE, encapsulation efficiency.

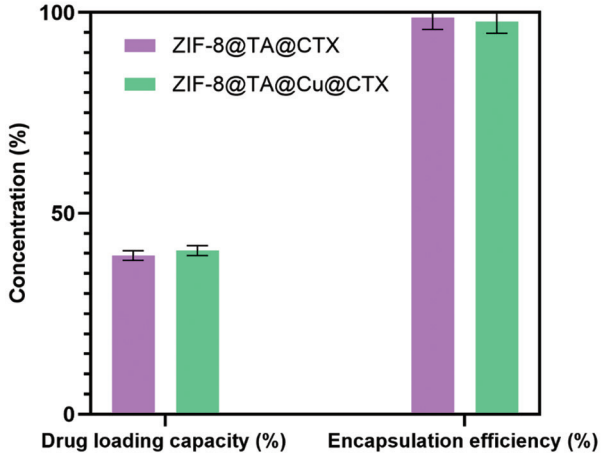

Figure 5. Concentration of DL and EE for CTX.

CTX, cefotaxime; DL, drug loading; EE, encapsulation efficiency.

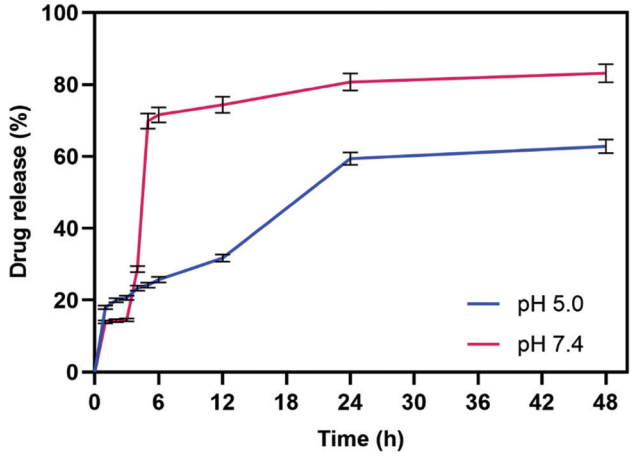

Figure 6. Cumulative release of CTX from ZIF-8@TA@Cu@CTX in acetate (pH 5.0) and phosphate buffer (pH 7.4) solutions.

CTX, cefotaxime; TA, tannic acid; ZIF, zeolitic imidazolate framework.

CTX and 3223 ± 293 nm and PDI: 0.36 ± 0.09 for ZIF-8@TA@Cu@CTX). Secondary aggregates may influence mass transfer and biological interactions, as suggested by micron-scale hydrodynamic diameters.

Loading capacity and encapsulation efficacy of CTX

CTX loading in ZIF-8 MOFs was measured using an indirect method. The EE and DLC were determined using a standard curve with the range of 3.96–23.76 µg/mL, as illustrated in Figure 4. The limit of detection and limit of quantification of the method were 1.10 and 3.33 µg/mL, respectively. The DLC and EE were detected as 39.50 ± 1.19% and 98.75 ± 2.96% for ZIF-8@TA@CTX, respectively, while they were 40.75 ± 1.22% and 97.75 ± 2.93% for ZIF-8@TA@Cu@CTX, respectively (Figure 5).

Determination of MIC and MBC

The in vitro antimicrobial activity of the DDSs against five gram-negative bacteria and four gram-positive bacteria determined by the dilution technique using CLSI recommendations. Table 1 presents the results of the antimicrobial experiments for all samples.

The test cultures, *Pseudomonas aeruginosa* American Type Culture Collection (ATCC) 27853 and *Escherichia coli* ATCC 25922, demonstrated resistance to all synthesized ZIF-8 MOFs. Among the DDSs tested, only ZIF-8@TA@Cu showed antimicrobial activity against both Proteus vulgaris ATCC 13315 and methicillin-resistant *S. aureus* (MRSA) ATCC 43300 with MIC values of 1250 µg/mL and 312.5 µg/mL, respectively. ZIF-8@TA@Cu@CTX had the lowest MIC activity with 312.5 µg/mL against *Klebsiella pneumoniae* ATCC 4352 among gram-negative bacteria.

All DDSs except for ZIF-8 showed good activity against *S. aureus*, with an MIC value of 39.06 (DDSs except for ZIF-8 and last one in Table 1) and 19.53 g/mL (for ZIF-8@TA@Cu@CTX) 19.53 µg/mL. Besides, ZIF-8@TA@CTX, and ZIF-8@TA@Cu@CTX had the same inhibitory activity against *Staphylococcus epidermidis* ATCC 12228 with an MIC value of 19.53 µg/mL. The

MBC values of the DDSs were found against *S. aureus* ATCC, *S. epidermidis* ATCC 12228, and *Enterococcus faecalis* ATCC 29212 among Gram-positive bacteria, and ZIF-8, ZIF-8@TA, and ZIF-8@TA@Cu@CTX exhibited the lowest MBC values against *S. epidermidis* ATCC 12228 (Table 2).

The drug release profile of ZIF-8@TA@Cu@CTX in acetate (pH 5.0) and phosphate buffer (pH 7.4) solutions at 37 ± 0.5˚ C is shown in Figure 6. The quantity of drug released was calculated based on the analytical curve. Within the first six hours, CTX release from ZIF-8@TA@Cu@CTX was observed to be 25.78 ± 0.77% in a pH 5.0 acetate buffer, while the cumulative drug release was determined to be 71.64 ± 2.15% in a pH 7.4 phosphate buffer. Following a 48-hour period, the percentage of drug release was 62.83 ± 1.89% at pH 5.0 and 83.19 ± 2.50% at pH 7.4.

The release pattern data were processed using GraphPad Prism software to analyze the mechanism of drug release kinetics. The parameters of each model are shown in Table 3. The *in vitro* dissolution rate results were best fitted Korsmeyer–Peppas kinetics model (Figure 7), which yielded the highest R^2 value in both dissolution media.

DISCUSSION

Recently, there has been a mounting interest in the use of MOF-based DDSs as a means of combating antibiotic resistance. ZIF-8 offers a highly porous delivery system and has antibacterial and anti-inflammatory properties due to the presence of Zn^{+2} ions in its composition.[33] For example, Costa et al.[2] combined ZnO nanoparticles with ZIF-8 and loaded them

Table 1. MIC (mg/L) of synthesized DDSs against gram-negative and gram-positive bacteria.

Synthesized DDSs	*P. aeruginosa* ATCC 27853	*E. coli* ATCC 25922	*K. pneumoniae* ATCC 4352	*P. vulgaris* ATCC 13315	*E. faecalis* ATCC 29212	*S. epidermidis* ATCC 12228	*S. aureus* ATCC 29213	*A. baumannii* ATCC 19606	MRSA ATCC 43300
ZIF-8	-	-	-	-	625	39.06	156.25	625	-
ZIF-8@TA	-	-	625	-	625	39.06	39.06	625	-
ZIF-8@TA @Cu	-	-	625	1250	625	39.06	39.06	625	312.5
ZIF-8@TA @CTX	-	-	625	-	625	19.53	39.06	625	-
ZIF-8@TA @Cu@CTX	-	-	312.5	-	156.25	19.53	19.53	625	-
CTX	8	0.125	0.060	16	1	1	1	16	4
Reference	0.5[a]	0.06[a]	0.5[a]	0.125[a]	2[a]	0.25[a]	0.06[a]	0.5[a]	1[b]

[a]Meropenem; [b]Ciprofloxacin. ATCC, American Type Culture Collection; CTX, cefotaxime; DDSs, drug delivery systems; MIC, minimum inhibitory concentration; MRSA, methicillin-resistant *S. aureus*; TA, tannic acid; ZIF, zeolitic imidazolate framework.

Table 2. MBC (mg/L) of synthesized DDSs against gram-negative and gram-positive bacteria.

Synthesized DDSs	*P. aeruginosa* ATCC 27853	*E. coli* ATCC 25922	*K. pneumoniae* ATCC 4352	*P. vulgaris* ATCC 13315	*E. faecalis* ATCC 29212	*S. epidermidis* ATCC 12228	*S. aureus* ATCC 29213	A. baumannii ATCC 19606	MRSA ATCC 43300
ZIF-8	-	-	-	-	625	39.06	625	-	-
ZIF-8@TA	-	-	-	-	625	78.12	1250	-	-
ZIF-8 @TA @Cu	-	-	-	1250	625	312.5	625	-	-
ZIF-8 @ TA @ CTX	-	-	-	-	625	312.5	1250	-	-
ZIF-8 @TA @Cu@CTX	-	-	-	-	156.25	19.53	1250	-	-
CTX	8	0.6	0.06	16	1	1	2	32	8
Reference	0.5[a]	0.06[a]	0.5[a]	0.125[a]	2[a]	0.25[a]	0.06[a]	0.5[a]	1[b]

[a]Meropenem; [b]Ciprofloxacin. ATCC, American Type Culture Collection; CTX, cefotaxime; DDSs, drug delivery systems; MBC, minimum bactericidal concentration; MRSA, methicillin-resistant *S. aureus*; TA, tannic acid; ZIF, zeolitic imidazolate framework.

Table 3. Drug release kinetic model parameters for ZIF-8@TA@Cu@CTX.

Sample name	Zero order		First order		Higuchi		Korsmeyer–Peppas	
	R^2	K_0	R^2	K_1	R^2	K_h	R^2	n
pH 5.0	0.848	1.083	0.749	-0.024	0.895	10.31	0.908	0.472
pH 7.4	0.446	32.49	0.366	-0.019	0.580	15.98	0.729	0.614

CTX, cefotaxime; TA, tannic acid; ZIF, zeolitic imidazolate framework.

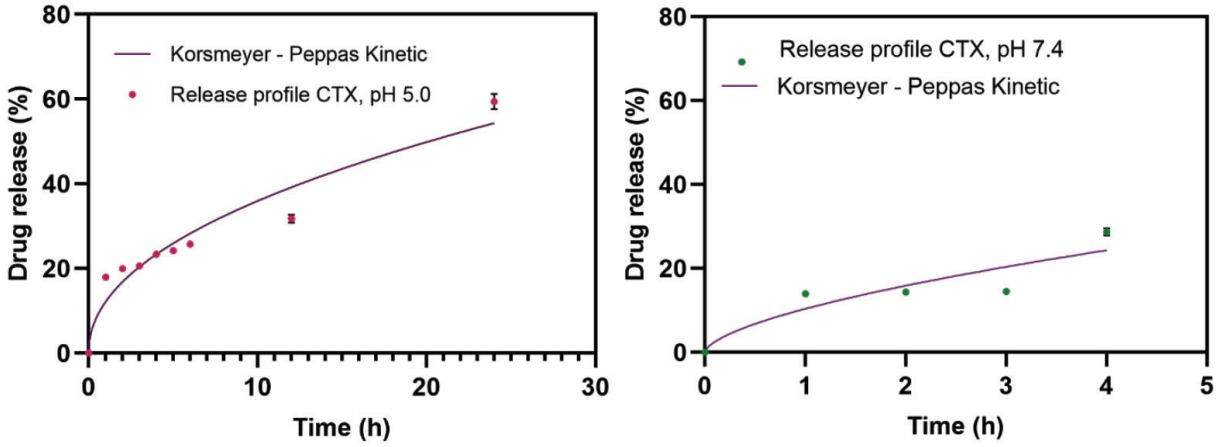

Figure 7. Korsmeyer–Peppas kinetics model fitting curves of DDS in acetate (pH 5.0) and phosphate buffer (pH 7.4) solutions.
CTX, cefotaxime; DDSs, drug delivery systems.

with the antibiotic ciprofloxacin to increase their antimicrobial activity through synergistic efficacy. They concluded that the combination of CIP and ZnO@ZIF-8 reduced the amount of CIP required to achieve an MIC similar to that of pure ciprofloxacin.[2]

In this study, ZIF-8 MOF was successfully synthesized and modified with TA and Cu by incorporating antimicrobial CTX. As seen in Figure 2 the formation of ZIF-8 MOF, surface modifications, and DL were confirmed by the functional groups and stretching vibrations in the 4000-400 cm^{-1} spectra. This was further validated using zeta potential measurements. The difference in surface charge illustrated that the compounds (e.g., TA and Cu ions) were successfully loaded on the ZIF-8 MOF surface (Figure 3). The absolute potential increased when TA was bonded to the ZIF-8 surface due to the -OH moieties, whereas it decreased when Cu ions were attached due to their positive charge.

Owing to the large cages of ZIF-8 MOFs,[2] the DLC values (39.50% for ZIF-8@TA@CTX and 40.75% for ZIF-8@TA@Cu@CTX) were quite consistent with the literature.

It was initially anticipated that CTX release would be higher under acidic conditions (pH 5.0 acetate buffer), considering the pH-sensitive nature of ZIF-8 and the protonation-induced weakening of coordination between imidazole ligands and Zn^{2+} ions.Therefore, acidic environments are commonly associated with ZIF-8 degradation and drug release.[34] However, the experimentally observed higher drug release at pH 7.4 phosphate buffer can be explained by the specific role of phosphate ions present in the dissolution medium. As previously reported by Velásquez-Hernández et al.,[35] phosphate species exhibit a strong affinity toward Lewis acidic metal centers such as Zn^{2+}, effectively competing with imidazole ligands and accelerating framework decomposition in PBSs. This ligand-exchange process leads to ZIF-8 structural disruption and promotes rapid drug liberation, accompanied by the formation of insoluble zinc phosphate species.[35] Accordingly, the pronounced burst release observed in the pH 7.4 medium during the initial hours can be attributed to phosphate-induced ZIF-8 degradation rather than to pH effects alone. In contrast, no abrupt framework collapse was observed under acidic but phosphate-free conditions (pH 5.0 acetate buffer), resulting in a more gradual and sustained release profile extending up to 48 h.

In addition to chemical and buffer-dependent factors, the particle size may contribute to the observed release behavior. Measurements of the rehydrated formulations revealed hydrodynamic diameters in the micron range, indicating the formation of secondary aggregates upon re-dispersion. Such aggregation, which can be promoted by multidentate interactions of TA and further enhanced by Cu^{2+}-mediated interparticle bridging, may reduce the available effective surface area for mass transfer.[19,36] Moreover, micron-scale hydrodynamic sizes can limit immediate particle–bacteria contact, which has been reported to contribute to sustained drug release behavior and to restrict the apparent enhancement of antimicrobial potency observed in MIC and MBC assays for nanoparticle-based antibiotic delivery systems.[37,38]

Overall, these findings indicate that drug release from ZIF-8-based DDSs is governed not only by pH sensitivity but also by buffer composition and the rehydrated system's physical state.

While the faster release observed at pH 7.4 may be attributed to phosphate-induced framework destabilization, the sustained release under mildly acidic, phosphate-free conditions could result from controlled framework degradation combined with diffusion through the MOF structure. In addition, the micron-scale hydrodynamic sizes observed after rehydration may contribute to prolonged release by limiting the effective surface area and mass transfer. Taken together, these characteristics support the potential applicability of ZIF-8-based DDSs for infection-associated environments, which are often characterized by local acidosis.[39]

As given in the Korsmeyer–Peppas equation, n denotes the release exponent, where if n ≤0.45, the release is controlled by Fickian diffusion. Values ranging from 0.45 to 0.89 indicate a non-Fickian diffusion process, whereas values greater than 0.89 correspond to case-II transport or zero-order (swelling-driven) release.[40] n is a useful indicator to determine the release mechanism. The release exponent increased from 0.472 at pH 5.0 to 0.614 at pH 7.4 when the Korsmeyer–Peppas model was applied to the initial release region of ≤60%. The value at pH 5.0 indicates a diffusion-dominated early release with minor deviations from ideal Fickian behavior, possibly resulting from drug desorption from the ZIF-8 cages and subsequent CTX diffusion through the MOF structure. Conversely, higher n values at pH 7.4 indicate anomalous transport, which is consistent with the contribution of phosphate-induced framework destabilization in addition to diffusion.[41] Therefore, it appears that the early release of CTX in phosphate buffer is governed by coupled diffusion and matrix disruption processes, whereas a more diffusion-controlled profile is maintained under acidic, phosphate-free conditions.

The CTX release profile revealed a pronounced initial release, particularly at physiological pH, followed by a sustained release phase. Although such release behavior could be expected to support antibacterial activity, the MIC or MBC values of the CTX-loaded DDSs were not lower than those of free CTX. This outcome suggests that antibacterial performance is influenced by factors beyond the overall amount of drug released.[42] Despite the inherent antibacterial properties of TA and Cu^{2+} ions, their incorporation into ZIF-8 predominantly results in their coordination or surface association, thereby constraining their direct and independent interaction with bacterial cells under MIC and MBC testing conditions. Although CTX was released in substantial amounts as detected by the analytical method, transient interactions with Zn^{2+}/Cu^{2+} ions and TA may reduce the fraction of freely available and biologically active drug during early exposure.[43] In parallel, non-covalent interactions between CTX and polyphenolic compounds, such as TA, may transiently influence the fraction of pharmacologically active drugs during early exposure.

Furthermore, the local microenvironment generated during the partial degradation of the ZIF-8 framework, including transient metal ion release and local coordination effects, may influence the immediate availability of CTX for bacterial targets rather than causing chemical degradation of the drug. Such effects are of particular relevance to β-lactam antibiotics, whose antibacterial activity depends on the freely accessible fraction of the drug during early exposure rather than on the total drug concentration.[44]

The findings of this study indicate that the ZIF-8-based DDS is not primarily designed to surpass free CTX in short-term *in vitro* assays, but rather to provide controlled delivery and prolonged local exposure. Therefore, the observed antibacterial behavior reflects the balance between release kinetics, drug–carrier interactions, and microenvironmental factors, rather than an unexpected loss of antimicrobial efficacy. It is also important to note that the MIC and MBC assays are based on short-term exposure and, therefore, may not fully capture the potential benefits of SR formulations, especially in the context of localized infection.

From a clinical perspective, the ZIF-8-based DDS was not primarily intended to reduce the systemic dose of CTX but rather to modulate its local availability through controlled release. This approach may be of particular relevance in cases of localized infections, where prolonged exposure at the infection site could enhance antibacterial efficacy. With regard to safety considerations, Cu^{2+} ions were incorporated into the DDS in a coordinated state within the ZIF-8 framework, which may limit the immediate availability of free Cu^{2+} ions under physiological conditions. However, further detailed *in vivo* investigations are required to comprehensively evaluate copper biodistribution, toxicity, and clearance. In conclusion, while the present study provides proof-of-concept *in vitro* findings, further *in vivo* studies are required to more accurately assess the system's translational potential.

CONCLUSION

In this study, a ZIF-8-based MOF DDS was successfully synthesized and further modified with TA and Cu ions. The high porous nature of the ZIF-8 framework enabled efficient DL and EE of CTX. Although the TA- and Cu-modified ZIF-8 DDSs did not enhance the antimicrobial potency of CTX in terms of MIC and MBC values compared to free drug, they preserved bactericidal activity under sustained exposure conditions.

Drug release studies revealed biphasic behavior, which is governed by pH and buffer composition. Phosphate-induced framework destabilization led to accelerated release at pH 7.4, whereas a more gradual, sustained release profile was observed in an acetate buffer at pH 5.0. The prolonged release of CTX for up to 48 h under mildly acidic conditions without abrupt framework collapse suggests that ZIF-8-based maintain controlled local drug availability in microbial infection-relevant environments.

TA and Cu modification primarily contribute to the observed release behavior and carrier characteristics by modulating the coordination environment and surface interactions within the ZIF-8 framework, rather than directly enhancing the antimicrobial potency. Therefore, the ZIF-8 MOF system represents a promising platform for controlled and localized antibiotic delivery, particularly for applications where prolonged exposure at infection sites is desirable, while acknowledging that further *in vivo* investigations are required to assess

translational potential and safety.

Ethics

Ethics Committee Approval: There is no require for ethical approval.

Informed Consent: Not required.

Acknowledgements

The authors would like to express their gratitude to Prof. Dr. Mahmut Özacar for granting them access to the laboratory infrastructure and for his invaluable assistance throughout this study.

Footnotes

Authorship Contributions

Surgical and Medical Practices: Y.P.T., M.Ö., D.D.Ç., Concept: M.Ö., D.D.Ç., Design: M.Ö., D.D.Ç., Data Collection or Processing: Y.P.T., M.Ö., D.D.Ç., Analysis or Interpretation: Y.P.T., D.D.Ç., Literature Search: Y.P.T., M.Ö., D.D.Ç., Writing: Y.P.T., D.D.Ç.

Conflict of Interest: The authors declare no conflicts of interest.

Financial Disclosure: The authors declared that this study received no financial support.

REFERENCES

1. AlQurashi DM, AlQurashi TF, Alam RI, Shaikh S, Tarkistani MAM. Advanced nanoparticles in combating antibiotic resistance: current innovations and future directions. J Nanotheranostics. 2025;6:9.
2. Costa BA, Abuçafy MP, Barbosa TWL, da Silva BL, Fulindi RB, Isquibola G, da Costa PI, Chiavacci LA. ZnO@ZIF-8 nanoparticles as nanocarrier of ciprofloxacin for antimicrobial activity. Pharmaceutics. 2023;15:259.
3. Endale H, Mathewos M, Abdeta D. Potential causes of spread of antimicrobial resistance and preventive measures in One Health perspective: a review. Infect Drug Resist. 2023;16:7515-7545.
4. Muteeb G, Rehman MT, Shahwan M, Aatif M. Origin of antibiotics and antibiotic resistance, and their impacts on drug development: a narrative review. Pharmaceuticals (Basel). 2023;16:1615.
5. Al Hagbani T, Rizvi SMD, Hussain T, Mehmood K, Rafi Z, Moin A, Abu Lila AS, Alshammari F, Khafagy ES, Rahamathulla M, Abdallah MH. Cefotaxime mediated synthesis of gold nanoparticles: characterization and antibacterial activity. Polymers (Basel). 2022;14:771.
6. Mihaiescu DE, Istrati D, Morosan A, Stanca M, Purcareanu B, Cristescu R, Vasile BS, Trusca RD. Low release study of cefotaxime by functionalized mesoporous silica nanomaterials. Gels. 2022;8:711.
7. Johnson JK, Laughon MM. Antimicrobial agent dosing in infants. Clin Ther. 2016;38:1948-1960.
8. Javaid S, Ahmad NM, Mahmood A, Nasir H, Iqbal M, Ahmad N, Irshad S. Cefotaxime loaded polycaprolactone based polymeric nanoparticles with antifouling properties for *in-vitro* drug release applications. Polymers (Basel). 2021;13:2180.
9. Mir RA, Weppelmann TA, Teng L, Kirpich A, Elzo MA, Driver JD, Jeong KC. Colonization dynamics of cefotaxime resistant bacteria in beef cattle raised without cephalosporin antibiotics. Front Microbiol. 2018;9:500.
10. Mir RA, Weppelmann TA, Johnson JA, Archer D, Morris JG, Jeong KC. Identification and characterization of cefotaxime resistant bacteria in beef cattle. PLoS One. 2016;11:e0163279.
11. Parvin N, Joo SW, Mandal TK. Nanomaterial-based strategies to combat antibiotic resistance: mechanisms and applications. Antibiotics (Basel). 2025;14:207.
12. Hameed S, Sharif S, Ovais M, Xiong H. Emerging trends and future challenges of advanced 2D nanomaterials for combating bacterial resistance. Bioact Mater. 2024;38:225-257.
13. Aflakian F, Mirzavi F, Aiyelabegan HT, Soleimani A, Navashenaq JG, Karimi-Sani I, Zomorodi AR, Vakili-Ghartavol R. Nanoparticles-based therapeutics for the management of bacterial infections: a special emphasis on FDA approved products and clinical trials. Eur J Pharm Sci. 2023;188:106515.
14. Mendez-Pfeiffer P, Monrreal MGB, Mendez-Encinas MA, Valencia D, Ortiz B, González-Davis O, Cadena-Nava RD. Nanoparticles in antibacterial therapy: a systematic review of enhanced efficacy against intracellular bacteria. ACS Omega. 2025;10:17070-17086.
15. Ohsaki S, Satsuma H, Nakamura H, Watano S. Improvement of solubility of sparingly water-soluble drug triggered by metal-organic framework. J Drug Deliv Sci Technol. 2021;63:102490.
16. Özsoy M, Pirincci Tok Y, Guney Eskiler G, Tok F, Karakus S, Ozsoy Y, Özacar M. The lenalidomide derivative loaded and quercetin modified MIL-100 based novel drug delivery system for breast cancer treatment. J Drug Deliv Sci Technol. 2025;108:106923.
17. Arunkumar T, Castelino E, Lakshmi T, Mulky L, Selvanathan SP, Tahir M. Metal-organic frameworks in antibacterial disinfection: a review. ChemBioEng Rev. 2024;11:e202400006.
18. Yan L, Gopal A, Kashif S, Hazelton P, Lan M, Zhang W, Chen X. Metal organic frameworks for antibacterial applications. Chem Eng J. 2022;435:134975.
19. Wang Y, Tang Y, Guo L, Yang X, Wu S, Yue Y, Xu C. Recent advances in zeolitic imidazolate frameworks as drug delivery systems for cancer therapy. Asian J Pharm Sci. 2025;20:101017.
20. Altun S, Çakıroğlu B, Özacar M, Özacar M. A facile and effective immobilization of glucose oxidase on tannic acid modified $CoFe_2O_4$ magnetic nanoparticles. Colloids Surf B Biointerfaces. 2015;136:963-970.
21. Chevallier P, Wiggers HJ, Copes F, Zorzi Bueno C, Mantovani D. Prolonged antibacterial activity in tannic acid-iron complexed chitosan films for medical device applications. Nanomaterials (Basel). 2023;13:484.
22. Bisht N, Dwivedi N, Kumar P, Venkatesh M, Yadav AK, Mishra D, Solanki P, Verma NK, Lakshminarayanan R, Ramakrishna S, Mondal DP, Srivastava AK, Dhand C. Recent advances in copper and copper-derived materials for antimicrobial resistance and infection control. Curr Opin Biomed Eng. 2022;24:100408.
23. Yu J, Huang X, Ren F, Cao H, Yuan M, Ye T, Xu F. Application of antimicrobial properties of copper. Appl Organomet Chem. 2024;38:e7506.
24. Ozsoy M, Atiroglu V, Guney Eskiler G, Atiroglu A, Arabaci G, Ozacar M. Activities of gallic acid and Fe doped, and glucose oxidase or gold modified ZIF-8 based drug delivery systems in triple negative breast cancer. J Drug Deliv Sci Technol. 2023;87:104878.
25. Resen AK, Atiroğlu A, Atiroğlu V, Guney Eskiler G, Aziz İH, Kaleli S, Özacar M. Effectiveness of 5-fluorouracil and gemcitabine hydrochloride loaded iron-based chitosan-coated MIL-100 composite as an advanced, biocompatible, pH-sensitive and smart drug delivery system on breast cancer therapy. Int J Biol Macromol. 2022;198:175-186.
26. Trucillo P. Drug carriers: a review on the most used mathematical models for drug release. Processes. 2022;10:1094.

27. Pirincci Tok Y, Mesut B, Güngör S, Sarıkaya AO, Aldeniz EE, Dude U, Özsoy Y. Systematic screening study for the selection of proper stabilizers to produce physically stable canagliflozin nanosuspension by wet milling method. Bioengineering (Basel). 2023;10:927.

28. Clinical and Laboratory Standards Institute. Methods for dilution antimicrobial susceptibility tests for bacteria that grow aerobically. Wayne (PA): CLSI; 2006.

29. National Committee for Clinical Laboratory Standards. Methods for determining bactericidal activity of antimicrobial agents: approved guideline M26-A. Wayne (PA): NCCLS; 1999.

30. Kaur H, Mohanta GC, Gupta V, Kukkar D, Tyagi S. Synthesis and characterization of ZIF-8 nanoparticles for controlled release of 6-mercaptopurine drug. J Drug Deliv Sci Technol. 2017;41:106-112.

31. El-Damhougy TK, Ahmed ASI, Gaber GA, Mazied NA, Bassioni G. Radiation synthesis for a highly sensitive colorimetric hydrogel sensor-based p(AAc/AMPS)-TA for metal ion detection. Results Mater. 2021;9:100169.

32. Latrach Z, Moumen E, Kounbach S, El Hankari S. Mixed-ligand strategy for the creation of hierarchical porous ZIF-8 for enhanced adsorption of copper ions. ACS Omega. 2022;7:15862-15869.

33. Khafaga DSR, El-Morsy MT, Faried H, Diab AH, Shehab S, Saleh AM, Ali GAM. Metal-organic frameworks in drug delivery: engineering versatile platforms for therapeutic applications. RSC Adv. 2024;14:30201-30229.

34. Yang S, Lü F, Wang L, Liu S, Wu Z, Cheng Y, Liu F. pH-responsive metal-organic framework for targeted delivery of fungicide, release behavior, and sustainable plant protection. Molecules. 2024;29:5330.

35. Velásquez-Hernández MJ, Ricco R, Carraro F, Limpoco FT, Linares-Moreau M, Leitner E, Wiltsche H, Rattenberger J, Schröttner H, Frühwirt P, Stadler EM, Gescheidt G, Amenitsch H, Doonan CJ, Falcaro P. Degradation of ZIF-8 in phosphate buffered saline media. CrystEngComm. 2019;21:4538-4544.

36. Li D, Li J, Wang S, Wang Q, Teng W. Dually crosslinked copper-poly(tannic acid) nanoparticles with microenvironment-responsiveness for infected wound treatment. Adv Healthc Mater. 2023;12:e2203063.

37. Xiong MH, Bao Y, Yang XZ, Zhu YH, Wang J. Delivery of antibiotics with polymeric particles. Adv Drug Deliv Rev. 2014;78:63-76.

38. Razei A, Cheraghali AM, Saadati M, Fasihi Ramandi M, Panahi Y, Hajizadeh A, Siadat SD, Behrouzi A. Gentamicin-loaded chitosan nanoparticles improve its therapeutic effects on Brucella-infected J774A.1 murine cells. Galen Med J. 2019;8:e1296.

39. Ahmed SA, Hasan N, Bagchi D, Altass HM, Morad M, Althagafi II, Hameed AM, Sayqal A, Khder AERS, Asghar BH, Katouah HA, Pal SK. Nano-MOFs as targeted drug delivery agents to combat antibiotic-resistant bacterial infections. R Soc Open Sci. 2020;7:200959.

40. Nabipour H, Aliakbari F, Volkening K, Strong MJ, Rohani S. Novel metal-organic framework coated with chitosan-κ-carrageenan as a platform for curcumin delivery to cancer cells. Int J Biol Macromol. 2025;301:140027.

41. Stiepel RT, Pena EP, Ehrenzeller SA, Gallovic MD, Lifshits LM, Genito CJ, Bachelder EM, Ainslie KM. A predictive mechanistic model of drug release from surface eroding polymeric nanoparticles. J Control Release. 2022;351:883-895.

42. Pelgrift RY, Friedman AJ. Nanotechnology as a therapeutic tool to combat microbial resistance. Adv Drug Deliv Rev. 2013;65:1803-1815.

43. Lemire JA, Harrison JJ, Turner RJ. Antimicrobial activity of metals: mechanisms, molecular targets and applications. Nat Rev Microbiol. 2013;11:371-384.

44. Levison ME, Levison JH. Pharmacokinetics and pharmacodynamics of antibacterial agents. Infect Dis Clin North Am. 2009;23:791-815.